Segmental Motions of *cis*-Polyisoprene in the Bulk State: Interpretation of Dielectric Relaxation Data

I. Bahar* and B. Erman

Polymer Research Center and School of Engineering, Bogazici University, Bebek 80815, Istanbul, Turkey

F. Kremer and E. W. Fischer

Max-Planck-Institut für Polymerforschung, Postfach 3148, 6500 Mainz, Germany

Received May 6, 1991; Revised Manuscript Received September 16, 1991

ABSTRACT: Dipolar correlation functions are calculated for *cis*-polyisoprene in the bulk state. The time decay of the correlation functions results from the orientational motion of dipole moments accompanying the configurational transitions of the chain backbone. Examination of the intramolecular conformational energetics of the chain reveals that the transitions between rotational isomeric states takes place through coupled motion of triplets of neighboring bonds in the repeat units. The intermolecular effect on local chain dynamics is included in two stages: First, the relaxation in a homogeneous environment is treated through adoption of a local effective frictional resistance, increasing with the size of the kinetic segment. Second, two dynamically distinct environmental states representative of the free volume or density fluctuations of the medium are considered. The frequency distribution of relaxational modes is found to broaden with increasing number of bonds cooperatively participating in the segmental mode process. Calculations are performed for different sizes of kinetic segments which are defined as a sequences of bonds cooperatively participating in local relaxation. Predictions of the theory are compared with recent dielectric measurements (Boese, D.; Kremer, F. *Macromolecules* **1990**, *23*, 829) of bulk *cis*-polyisoprene. Calculations indicate that the experimentally observed Kohlrausch-Williams-Watts (KWW) exponent of 0.39 is reproduced when a kinetic segment of three repeat units cooperatively relaxing in the presence of free volume fluctuations of the environment is considered.

Introduction

Dielectric relaxation measurements[1-6] on *cis*-polyisoprene (*cis*-PIP) chains in the bulk state exhibit the presence of two distinct modes of relaxation process: a segmental mode resulting from configurational transitions of a few monomeric repeat units and a normal mode associated with the long-wavelength motions of the chain. The two modes display clearly distinct features. Correlation times for the segmental mode are faster by a few orders of magnitude; they are independent of the molecular weight of the chain. Those for the normal mode scale with the second power of the molecular weight below a critical value M_c and with a 3.7 power above it.[6] The time decay values of the orientational correlation function $\phi(t)$ for both modes have been approximated for a variety of polymers by the empirical Kohlrausch-Williams-Watts (KWW) or the stretched exponential function[7]

$$\phi(t) = \exp[-(t/\tau)^{\beta}] \qquad (1)$$

where τ is a characteristic correlation time and the exponent β is less than unity. β for the segmental mode in *cis*-PIP is experimentally found to be 0.39 and is independent of temperature whereas it is larger than 0.5 for the normal mode and increases with temperature.[6]

As has first been discussed by Stockmayer,[8] the component of the dipole moment vector parallel to the chain contour results in the normal mode process. Dielectric relaxation associated with this component leads to information on the low frequency dynamics of the chain. The basic features of the normal mode process may be interpreted in terms of the Rouse and the reptation models[2,6] describing the dynamics of the end-to-end chain vector. In view of this correspondence, the parameters determining the normal mode process are expected to be universal and valid for the generic flexible polymer chain. The segmental mode, on the other hand, is associated with high frequency motions and depends strongly on the local chemical structure of the chain.

Segmental modes in the bulk *cis*-PIP have also been explored by time-resolved optical fluorescence[9] and carbon-13 NMR measurements,[10] in addition to dielectric relaxation experiments. The relation of local segmental dynamics to molecular constitution is not well established yet. In a recent study,[9] the use of the anisotropic rotational diffusion model of a rigid body is shown to be insufficient in describing the experimentally determined correlation functions for *cis*-PIP. The kinetic Ising model of Skinner[11] and Fredrickson and Brawer[12] and the model of viscous liquids proposed by Brawer[13] come closest to describing the cooperative nature of local dynamics. However, in those studies[10-12] the chain is represented in a very general way as a two-spin system of a one-dimensional Ising model. Models of such generality establish the qualitative aspects of the local dynamics such as the non-Arrhenius temperature dependence of relaxation times and nonexponential decay of correlation functions. The system-specific quantitative features of local dynamics, however, are not included in those treatments. In addition to the role of the single chain in dielectric relaxation, local density fluctuations also contribute to the nonexponential shape of the relaxation function. This is apparent from results of light scattering experiments on small molecules[14-16] leading to values of β in the range 0.38-0.62. One explanation for these values of the β parameter is the presence of spatial and temporal density fluctuations resulting in environmental heterogeneities for the relaxing dipoles, therefore leading to a spectrum of relaxation times.

0024-9297/92/2225-0816$03.00/0

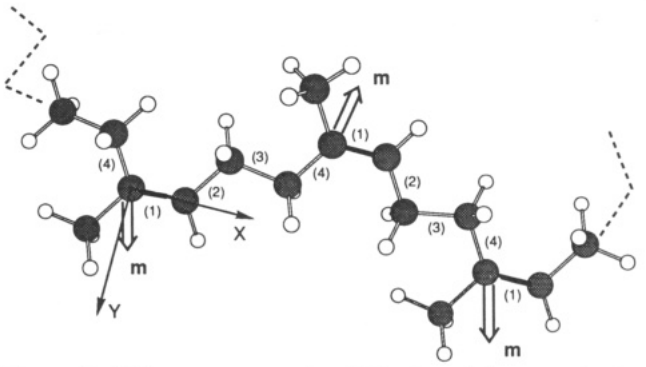

Figure 1. A few monomer units of the *cis*-polyisoprene chain. The shaded and the empty circles represent the carbon and the hydrogen atoms, respectively. The darker bonds represent the double bonds. The bonds of the monomer unit are numbered from 1 to 4. The x- and the y-axes of the reference coordinate system are affixed to the double bond as shown. The broken dashed lines represent the tails of the long chain. The dipole moments **m** are affixed to the first atom of the double bond.

The dynamic rotational isomeric state (DRIS) model, which has been developed over the past years[17-24] for investigating the sub-Rouse dynamics of polymers, is capable of incorporating the specific details of local structure into the kinetic Ising model in the presence of a fluctuating environment.

The aim of the present paper is to investigate the segmental mode relaxation process of *cis*-PIP chains in the bulk state above the glass transition temperature by the DRIS model. In the following section, we outline the assumptions of the model and the approximations involved. A convenient matrix multiplication scheme is outlined for the stochastic analysis of configurational transitions in the chain. As a first step, the orientational correlation functions are computed on the basis of intramolecular effects only. The environmental effect therein is approximated by a mean-field effective frictional resistance. This approach represents relaxation in a homogeneous environment and provides information on contributions from both single-chain connectivity and intramolecular energetics to the segmental mode relaxation processes of the chain. Relaxation in a heterogeneous environment results when the density of the melt exhibits spatial and temporal fluctuations. The effect of these fluctuations is included as a further step in the treatment. In Calculations and Discussion, predictions of the theory are compared with experiments.

Theory

DRIS Model and Assumptions. In this section we describe a model for analyzing the intramolecular contributions to segmental dielectric relaxation for the PIP chain. A small portion of a *cis*-PIP chain is shown in Figure 1. The remaining parts of the chain, which will be defined as the "tails", are indicated by the broken dashed lines. The repeat unit $-[C(CH_3)=CHCH_2CH_2]-$ consists of the four bonds numbered from 1 to 4 in parentheses in the figure. The first bond is a double bond. The shaded circles represent the carbon atoms. A molecule-fixed coordinate system OXYZ is affixed to the double bond. Following the convention adopted in the rotational isomeric state formalism of polymer statistics,[25] the X-axis is directed along the double bond. The Y-axis is taken to make an acute angle with the extension of the previous bond, and the Z-axis (not shown) completes a right-handed coordinate system. The dipole moment **m** of each repeat unit is indicated by an arrow affixed to the first carbon atom of the double bond.

The local dynamics of the chain results from configurational transitions of short sequences of bonds. The length of the sequence to be considered depends on the time scale of the specific experiment. In general, the sequence should be sufficiently large to allow for the cooperative rearrangement of the bonds participating in the segmental mode process. In the segmental relaxation process of PIP investigated by fluorescence spectroscopy, the length of the sequence is estimated to be on the order of a few monomer units.[9] The sequence of bonds cooperatively contributing to segmental relaxation will be referred to as the "kinetic segment" in the present work. Within the time scale of the experiments, the motions of the kinetic segment will be assumed to be dynamically uncorrelated with those of the tails. Thus, it suffices to explicitly formulate the correlation functions of the dipole moments within one kinetic segment only.

The bond rotameric transitions appear as jump processes where the bond oscillates around an isomeric minimum and occasionally jumps to another minimum. The rates of these transitions are assumed to take place according to Kramers' rate expression. The latter is given as the product of two terms, a front factor and an exponential activation energy term. The front factor represents the coupling of the chain to its environment. The activation energy term reflects the contributions to dynamics from intramolecular energetics.

A rotameric transition over a single bond will be possible only if several adjoining bonds within the kinetic segment can be cooperatively set in motion. We call this the chain connectivity effect. In the absence of inertial effects and friction from the surroundings, the tails of the kinetic segment may undergo large sweeping motions when a bond in the kinetic segment undergoes a rotameric transition. For a polymeric chain embedded in a dense surrounding on the other hand, such sweeping motions are not likely. Such motions are suppressed in the present model by introducing a position-dependent friction coefficient according to which the motion of a given point on the chain is damped out depending on its location relative to the bond initiating the rotameric transition.

We express the dynamics of all dipole moments relative to the coordinate system OXYZ, thereby identifying the latter as the laboratory-fixed coordinate system. The errors due to this approximation will be inconsequential if the damping effect of the environment is sufficiently strong, such as in the bulk state, and if we are observing the motions of the dipoles sufficiently separated from the origin. In any case, a correction may be applied by introducing independent overall motions to the coordinate system as has been discussed previously.[17]

Basic Approach. Master Equation Formalism. Let us assume that there are n bonds between the investigated dipole moment vector and the coordinate system OXYZ and that these bonds are capable of exhibiting transitions from one isomeric state to the other. A set of torsional angles $\{\Phi\}_\alpha = \{\phi_1, \phi_2, ..., \phi_n\}$ specifies any configuration α taken by the segment between the origin and the dipole moment. The subscript α in $\{\Phi\}_\alpha$ varies in the range $1 \leq \alpha \leq N$, where N denotes the total number of configurations. For example, if there are n rotatable bonds each having ν accessible isomeric states, then $N = \nu^n$. The aim of the DRIS model is to calculate the joint probability that the sequence under consideration is in the ith configuration at time zero and in the jth configuration at time t. We let $\mathbf{P}(t)$ represent the N-dimensional vector of the time-dependent probabilities for all possible configurations $\{\Phi\}_\alpha$.

$\mathbf{P}(t)$ obeys the master equation

$$\frac{d\mathbf{P}(t)}{dt} = \mathbf{A}\mathbf{P}(t) \tag{2}$$

where $\mathbf{A}$ is the $N \times N$ transition rate matrix for the segment. The element A_{kl} of $\mathbf{A}$ represents the rate constant for the passage from configuration $\{\Phi\}_l$ to $\{\Phi\}_k$. Equation 2 may be solved formally to yield

$$\mathbf{P}(t) = \exp(\mathbf{A}t)\,\mathbf{P}(0)$$
$$= \mathbf{B}\exp(\Lambda t)\,\mathbf{B}^{-1}\mathbf{P}(0) = \mathbf{C}(t)\,\mathbf{P}(0) \tag{3}$$

where $\mathbf{P}(0)$ is the array of the initial probabilities of the N accessible configurations, $\mathbf{B}$ is the matrix of eigenvectors of $\mathbf{A}$, Λ is the diagonal matrix of eigenvalues of $\mathbf{A}$, $\mathbf{B}^{-1}$ is the inverse of $\mathbf{B}$, and

$$\mathbf{C}(t) = \mathbf{B}\exp(\Lambda t)\,\mathbf{B}^{-1} \tag{4}$$

is the time-delayed conditional probability matrix with the elements $C_{\alpha\beta}$ describing the conditional probability of the occurrence of configuration $\{\Phi\}_\alpha$ at time t given the configuration $\{\Phi\}_\beta$ at time $t = 0$. The time-delayed joint probability matrix $\boldsymbol{P}(t)$ is obtained from $\mathbf{C}(t)$ as

$$\boldsymbol{P}(t) = \mathbf{C}(t)\ \mathrm{diag}\ \mathbf{P}(t{=}0) \tag{5}$$

Here diag $\mathbf{P}(t{=}0)$ is the diagonal matrix of the equilibrium probabilities $P(0)$.

The orientational correlation function $M_1(t)$ for any two vectors $\mathbf{m}$ and $\mathbf{n}$ follows from the ensemble average over all configurational transitions as

$$M_1(t) \equiv \langle \mathbf{m}(0)\cdot\mathbf{n}(t)\rangle = \sum_{\alpha=1}^{N}\sum_{\beta=1}^{N} \boldsymbol{P}_{\alpha\beta}(t)\,\mathbf{m}_\alpha\cdot\mathbf{n}_\beta \tag{6}$$

where the summations are performed over all configurations of the segment and $\mathbf{m}_\alpha$ and $\mathbf{n}_\beta$ denote the vectors $\mathbf{m}$ and $\mathbf{n}$ in the configurations α and β, respectively. In the following subsection, we describe the molecular structure and the energetics of the *cis*-PIP chain and then derive the corresponding rate matrix $\mathbf{A}$.

Torsional Energies, Isomeric Minima, and Saddle Points. The equilibrium statistics of PIP chains have been previously investigated by Mark[26] and Abe and Flory[27,28] by the rotational isomeric state formalism. The structure of the *cis*-PIP chain is shown in Figure 1. The conformational energetics of the chain is studied by considering the interaction potentials between pairs of nonbonded atoms, following conventional methods. Bond lengths are taken[27] as $l_{C-C} = 1.53$ Å, $l_{C-H} = 1.10$ Å, $l_{C'=C'} = 1.34$ Å, and $l_{C-C'} = 1.51$ Å, where C′ indicates the carbon atom next to the double bond. Supplemental bond angles equate[27] to $\angle C'C'C = 55°$, $\angle C'CC = 68°$, $\angle C'C'H = 61°$, and $\angle CC'(CH_3) = \angle C'CH = \angle CCH = 71°$. Lennard-Jones expressions

$$V_{kl} = a_{kl}/r_{kl}^{12} - b_{kl}/r_{kl}^{6} \tag{7}$$

are adopted in evaluating the interaction potential between atoms or groups k and l, separated by a distance r_{kl} from each other. The parameters a_{kl} and b_{kl} are found from the Slater–Kirkwood formula, using the structural variables listed in Table I. Intrinsic torsional potentials are accounted for (kcal/mol) by the expressions[25,27]

$$E_{\mathrm{intr}}(\phi_2,\phi_4) = 0.99(\cos(3\phi_2) + \cos(3\phi_4)) \tag{8}$$

$$E_{\mathrm{intr}}(\phi_3) = 1.4(1 - \cos(3\phi_3))$$

for the pair of bonds flanking the double bond and for the C–C bond, respectively.

Table I
Structural Variables for the Calculation of Lennard-Jones Parameters

atom/group	van der Waals radii (Å)	polarizability	N_e[a]
C	1.60	0.93	5.0
H	1.08	0.42	0.9
CH_3	1.80	1.77	7.0

[a] N_e = effective number of electrons in the outermost shell.

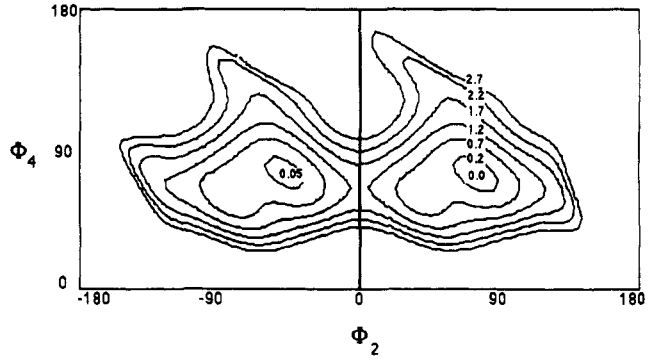

Figure 2. Energy contour maps for the two bonds flanking a double bond in the cis configuration. Two isomeric minima s^+s^+ and s^+s^- with respective energies of 0.00 and 0.05 kcal/mol are indicated. Six equally spaced contour levels ranging from 0.2 to 2.7 kcal/mol are drawn.

A segment of the form $CCH_2CH_2C(CH_3){=}CHCH_2C$ with the double bond in cis configuration ($\phi_1 = 180°$) has been considered as a first step to gain an understanding of the interdependence and kinetics of bond isomerization in *cis*-PIP. The energy contour diagram calculated as a function of the rotations ϕ_2 and ϕ_4 about the bonds adjoining the double bond is shown in Figure 2. Although this figure bears close resemblance with the equivalent map calculated by Abe and Mark, it is reevaluated in the present work in order to clarify the barriers between rotational isomeric states. The portion of the map for $0° \le \phi_4 \le 180°$ is shown only. The portion for $0° \ge \phi_4 \ge -180°$ is symmetric with respect to the origin. Energy levels are expressed in kilocalories/mole, with respect to the lowest minimum occurring near $\phi_2, \phi_4 = 80°, 75°$. The torsional angle ϕ_2 of the second minimum in the figure is slightly shifted toward the trans (t) state value, although the shape and depth of the isomeric minimum are closely preserved. In accordance with the previous treatment, neglecting those slight distortions, we can assume that rotations around the two bonds flanking a double bond are independent of each other and give rise to minimum energy states referred to as the skew[±] ($s^\pm$) states which are defined approximately by ±70° torsional angles with respect to the trans state. Another interesting feature revealed in calculations is that the fourth bond has to overcome an energy barrier of 4.5 kcal/mol for passage between the s^+ and s^- states. In view of the large value of this barrier, we assume that the passage from the s^+ to the s^- state for this bond is not possible. The second bond has to pass over a saddle point with a relatively low energy barrier of 1.4 kcal/mol on going from the s^+ to s^- state as seen from the figure. A more exact determination of the latter is possible by considering the interdependent behavior of triplets of single bonds in the repeat units, as presented next.

In contrast to the bonds flanking the double bond, the conformational behavior of triplets of single bonds 2–4 are found to be affected by second and higher order interactions along the chain.[24] Energy contour diagrams have been obtained for groups of triplewise dependent bonds by varying the torsional angles ϕ_2 and ϕ_3 while

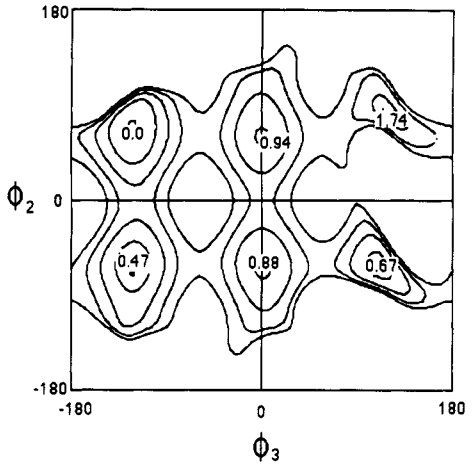

Figure 3. Energy contour map for the repeat unit in *cis*-PIP as a function of the torsional angles ϕ_2 and ϕ_3 of the second and the third bonds when the fourth bond is in the s^+ state. The energies of the minima are in kilocalories/mole. The contour lines are drawn at intervals of 1 kcal/mol.

keeping ϕ_4 fixed at either s^+ or s^- state in the segment $CC(CH_3)=CHCH_2CH_2C(CH_3)=CHC$. The energy contours shown in Figure 3 are obtained for the s^+ state of the fourth bond. For the s^- state of the latter bond, the mirror image of the figure is obtained and hence is not shown separately. The figure shows three isomeric states for the third bond, which may be identified as the trans (t) at $\phi_3 = 0°$ and gauche$^\pm$ ($g^\pm$) states at $\phi_3 = \pm 120°$. The energies of the isomeric minima are indicated in kilocalories/mole with respect to the lowest energy state; $\phi_2, \phi_3, \phi_4 = s^+g^-s^+$. The contours shown in the figure display isoenergetic points ranging from 1 to 4 kcal/mol, with intervals of 1 kcal/mol.

The energy map exhibits six minima and eight saddle-point passages as schematically represented by the arrows in Figures 4 for the cases where $\phi_3 = s^+$ and s^- (parts a and b, respectively). No passage between the two surfaces is accessible as delineated above. Also, the transitions which require substantially large activation energies, such as the passage from s^+ to s^- for the second bond when the third is in g^+ state, are indicated in the kinetic schemes with the infinity signs. The rate constants associated with the accessible transitions are indicated as $r_{\pm i}$ (i = 1–8). The corresponding activation energies $E_{\pm i}$ (i = 1–8) are calculated from the height of the saddles relative to the initial state and are listed in Table II. The set of $N = 12$ isomeric states available to each monomeric unit and the corresponding equilibrium energies which are denoted as E°_α (α = 1–12) are listed in Table III. Those states are assigned equilibrium probabilities p°_α equal to

$$p^\circ_\alpha = \exp(-E^\circ_\alpha/RT)/\sum_{\alpha=1}^{N} \exp(-E^\circ_\alpha/RT) \qquad (9)$$

For a segment of k repeat units, starting with the double bond, the equilibrium probability $\mathbf{P}_{\{\Phi\}}(t=0)$ of the configuration $\{\Phi\}$ is obtained from the serial multiplication of the equilibrium probabilities of the individual units in as much as units separated by a double bond are statistically independent.

Transition Rates. As stated in the Introduction, a rotameric transition about a bond results from diffusive motions of the bond about the energy minima or around the saddle point. During its rotameric oscillations about an isomeric minimum a bond may approach an activated state and eventually cross it to reach a new minimum energy state or it may move back to its original isomeric

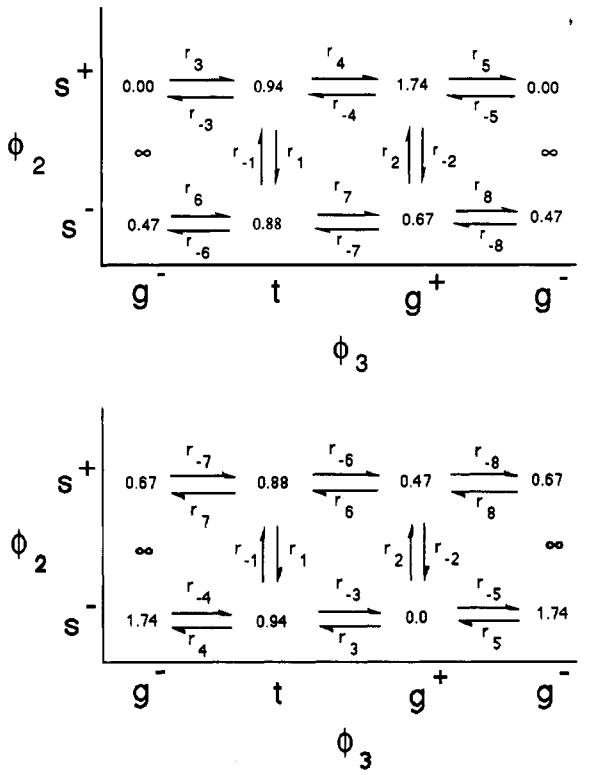

Figure 4. Schematic plot of rates of passage between different states accessible to the repeat unit in *cis*-PIP (a, top) when bond 4 is in the s^+ state and (b, bottom) when bond 4 is in the s^- state.

Table II
Activation Energies for the Various Rates (kcal/mol)

$E_1 = 1.88$	$E_5 = 1.44$	$E_{-1} = 1.82$	$E_{-5} = 3.18$
$E_2 = 1.90$	$E_6 = 3.40$	$E_{-2} = 2.37$	$E_{-6} = 2.99$
$E_3 = 3.73$	$E_7 = 2.45$	$E_{-3} = 2.79$	$E_{-7} = 2.66$
$E_4 = 2.56$	$E_8 = 3.04$	$E_{-4} = 1.76$	$E_{-8} = 3.24$

Table III
Rotational Isomeric States for Repeat Units and Corresponding Energies

states	energy (kcal/mol)
cs^+ts^+ and cs^-ts^-	0.94
$cs^+g^+s^+$ and $cs^-g^-s^-$	1.74
$cs^+g^-s^+$ and $cs^-g^+s^-$	0.00
cs^-ts^+ and cs^+ts^-	0.88
$cs^-g^+s^+$ and $cs^+g^-s^-$	0.67
$cs^-g^-s^+$ and $cs^+g^+s^-$	0.47

state. Thus, the local orientational dynamics of a polymeric chain proceeds in the form of jumps from one minimum to another. In general, these jumps take place collectively, as implicit in the discussion of Figure 3 where the transition of one bond from one minimum to another depends on the isomeric state of its neighboring bonds. The rate constant r_i for a rotameric transition over bond i is given by Kramers' high-friction limit expression as

$$r_i = \frac{(\gamma^*\gamma)^{1/2}}{2\pi\zeta_{i,\text{eff}}} \exp\{-E_i/RT\} \qquad (10)$$

where γ and γ^* refer to the curvature of the energy path at the minimum and saddle point, respectively, E_i is the activation energy for the specific transition, and $\zeta_{i,\text{eff}}$ is the effective friction coefficient for bond i. $\zeta_{i,\text{eff}}$ may be envisaged to contain information on the effect of the local environment of the bond. The intermolecular resistance to motion and the effect of local density or free volume fluctuations are accounted for in the front factor by suitably modifying the effective friction coefficient. The

Table IV
Rate Matrix for the Bond Triplet

	s^+ts^+	s^+ts^-	$s^+g^+s^+$	$s^+g^+s^-$	$s^+g^-s^+$	$s^+g^-s^-$	s^-ts^+	s^-ts^-	$s^-g^+s^+$	$s^-g^+s^-$	$s^-g^-s^+$	$s^-g^-s^-$
s^+ts^+		0	r_{-4}	0	r_3	0	r_1	0	0	0	0	0
s^+ts^-	0		0	r_6	0	r_{-7}	0	r_{-1}	0	0	0	0
$s^+g^+s^+$	r_4	0		0	r_{-5}	0	0	0	0	0	0	0
$s^+g^+s^-$	0	r_{-6}	0		0	r_8	0	0	0	r_{-2}	0	0
$s^+g^-s^+$	r_{-3}	0	r_5	0		0	0	0	0	0	r_2	0
$s^+g^-s^-$	0	r_4	0	r_{-8}	0		0	0	0	0	0	0
s^-ts^+	r_{-1}	0	0	0	0	0		0	r_{-7}	0	r_6	0
s^-ts^-	0	r_1	0	0	0	0	0		0	r_3	0	r_{-4}
$s^-g^+s^+$	0	0	0	0	0	0	r_4	0		0	r_{-8}	0
$s^-g^+s^-$	0	0	0	r_2	0	0	0	r_{-3}	0		0	r_5
$s^-g^-s^+$	0	0	0	0	r_{-2}	0	r_{-6}	0	r_8	0		0
$s^-g^-s^-$	0	0	0	0	0	0	0	r_4	0	r_{-5}	0	

magnitude of $\zeta_{i,\text{eff}}$ depends on the location of bond i within the kinetic segment. In as much as we are interested in the motions of a given dipole, the position of the bond performing the rotameric transition relative to the dipole is of importance. In general, the dynamics of the dipole moment will be less affected by the rotameric transitions about bonds that are at a larger distance along the chain than those relatively closer. Recent calculations[21] and their comparison with Brownian dynamics simulations[29] suggest that a quadratic dependence of $\zeta_{i,\text{eff}}$ on the number of intervening bonds between the dipole moment vector and the rotating bond is appropriate. Thus, the rate expression given by eq 10 will be written as

$$r_i = \frac{A_0(T)}{(n-i)^2} \exp\{-E_{act}/RT\} \qquad (11)$$

where n indicates the location of the dipole moment with respect to the origin and i that of the bond performing the rotameric transition. The various terms in the front factor of eq 10 are lumped into $A_0(T)$. The above equation deserves special attention. The exponential part arises from the specific chain conformational energetics whereas the term $(n-i)^{-2}$ may be viewed as a property common to all chainlike structure and responsible for the slowing and/or damping of the propagation of reorientation away from the rotating bond. Accordingly, r_i represents the effective rate constant associated with the motion of the dipole moment affixed to the nth bond as a result of the isomeric transition of bond i. It should be noted that the quadratic dependence of r_i on $(n-i)$ is not rigorously derived but only postulated on the basis of moment of inertia considerations and random-chain properties.[21] Although its adoption in previous work[21] leads to results in satisfactory qualitative agreement with Brownian simulations, further comparison with experiments and/or molecular dynamics simulations will be of interest to confirm the validity and limits of applicability of eq 11.

Transition Rate Matrices and Dispersion of Relaxational Modes. In the first part of the treatment below, we adopt a mean-field type analysis where the possible fluctuations and heterogeneities in the environment of the kinetic segment are not explicitly considered. Intermolecular effects are therefore included only through a single value of $\zeta_{i,\text{eff}}$ lumped into $A_0(T)$ in the front factor of eq 10. A large value of the front factor implicitly reflects the favorable cooperation of the surroundings to present suitable pathways to surmount the barrier to configurational transition. Conversely, low values of the front factor decrease the frequencies of jumps from one energy minimum to another. In this case, the kinetic segment in the investigated molecule is constrained to make many small fluctuations about a minimum energy configuration before hopping over the transition state to another isomeric state. The dielectric relaxation of the dipole results from the anisotropic intramolecular motions in such a homogeneous environment. It is noted that the orientational relaxation of a given vector along a chain cannot be obtained by a model based uniquely on local density fluctuations in as much as the latter is an isotropic process while the orientational relaxation is purely anisotropic. However, the contributions to dielectric relaxation from the nonhomogeneities of the fluctuating environment cannot be ignored totally because differences in the environment result in a wider spectrum of relaxation times and this directly influences the time decay of the relaxation function.

The boundary condition of immobilized tails is implicitly taken into account in the rate constants which are the elements of **A**, by decreasing the rate of reorientation of a given dipole with the second power of the number of intervening bonds between that dipole and the rotating bond i initiating the motion, according to eq 11. If the dipole is very close to the rotating bond, if it is its first neighbor along the chain (i.e., $n-i=1$), its motion exactly accompanies that of the rotating bond; otherwise, it is damped depending on its separation from the mobile unit.

In the second part of the analysis, we approximate the fluctuating environment as a two-state medium that may be referred to as a fast and a slow medium. This approximation has been employed by a number of investigators in previous studies.[30,31] Conformational transitions in the kinetic segment are more frequent in the fast environment compared to those in the slow medium. The correspondence of this model to density fluctuations is obvious. The fast and the slow states are not assumed to be static, and transitions from one state to the other are recognized. This model has recently been applied[20] to the analysis of the dynamics of small probes. In the present work, we extend this approach to kinetic segments of *cis*-PIP in heterogeneous environments.

(a) Relaxation of a Single Repeat Unit in a Homogeneous Environment. The rate matrix **A** accounting for the rotameric transitions of bonds in a repeat unit will be of order 12, in agreement with the number N of accessible configurations depicted in the kinetic scheme of Figure 4. The off-diagonal elements of the latter are listed in Table IV. The first row and column in the table indicate the set of initial and final states, respectively. The kth diagonal element of **A** represents the total rate of escape from state k. For stationary processes as presently considered, the diagonal elements are found from $A_{kk} = -\sum A_{lk}$, where the summation is performed over all states l different from k.

A total of $N=12$ relaxational modes with the frequencies λ_ξ $(1 \le \xi \le 12)$ deduced from the eigenvalues of **A** contributes to segmental motion of the repeat unit. In

component form, eqs 4 and 5 lead to the expression[19]

$$M_1(t) = \sum_{\xi=1}^{N} k_\xi \exp\{\lambda_\xi t\} \tag{12}$$

where the amplitude factor k_ξ is given by

$$k_\xi \equiv \sum_{\alpha=1}^{N}\sum_{\beta=1}^{N} [B_{\alpha\xi} B_{\xi\beta}^{-1} P_\beta(t=0)\ \mathbf{m}_\alpha\cdot\mathbf{n}_\beta] \tag{13}$$

(b) Relaxation of a Single Repeat Unit in a Fluctuating Environment. The rates of transitions between isomeric states are assumed to be affected by the state of the environment, but the reverse is not true; i.e., the isomeric state of the chain sequence does not affect the transition rate of the environment from the slow to the fast state. The fluctuating environment may be characterized by two parameters such as (i) the fraction p_{slow} of the slow state in the medium and (ii) the rate r_{slow} of transition from the slow to the fast state. The reverse transition rate r_{fast} is fixed by the detailed balance principle as

$$r_{slow}/r_{fast} = (1 - p_{slow})/p_{slow} \tag{14}$$

With the choice of two states for the environment, the total number of accessible states to a repeat unit in *cis*-PIP equates to 24. The transition rate matrix $\tilde{\mathbf{A}}$ of order 24 for that case reads

$$\tilde{\mathbf{A}} = \begin{bmatrix} \mathbf{A} r_{fast}\mathbf{E}_{12} & r_{slow}\mathbf{E}_{12} \\ r_{fast}\mathbf{E}_{12} & g\mathbf{A} - r_{slow}\mathbf{E}_{12} \end{bmatrix} \tag{15}$$

Here, $\mathbf{E}_{12}$ is the identity matrix of order 12, $\mathbf{A}$ is the transition rate matrix defined in Table IV, and the coefficient $g < 1$ accounts for the decreased mobility of the chain in the slow medium, relative to the fast medium. It equals the ratio of the values assumed by the effective friction coefficient $\zeta_{i,eff}$ in the slow and fast media.

(c) Relaxation of a Kinetic Segment of Several Repeat Units. In the more realistic case of x repeat units collectively participating in the relaxation process, the operating transition rate matrix $\mathbf{A}^{(x)}$ is found from the direct product of the individual transition matrices $\mathbf{A}$ (or $\tilde{\mathbf{A}}$) with identity matrices $\mathbf{E}_{12}$ of order 12, according to

$$\mathbf{A}^{(x)} \equiv \{\mathbf{A}_1 \otimes \mathbf{E}_{12} \otimes \mathbf{E}_{12} \dots \otimes \mathbf{E}_{12}\} + \{\mathbf{E}_{12} \otimes \mathbf{A}_2 \otimes \mathbf{E}_{12} \dots \otimes \mathbf{E}_{12}\} + \dots + \{\mathbf{E}_{12} \otimes \mathbf{E}_{12} \otimes \mathbf{E}_{12} \dots \otimes \mathbf{A}_x\} \tag{16}$$

Here, the subscripts 1, 2, ..., x are appended to $\mathbf{A}$ to distinguish between consecutive transition matrices, in as much as the front factor in the rate constants varies depending on the position (n) of the investigated vector relative to the bond i ($1 \le i \le n = 4x$) undergoing the rotameric transition, as given by eq 11. Accordingly, as x increases, increasingly slower modes contribute to the segmental relaxation process. The orientational correlation is still given by a sum of exponentials as represented by eqs 12 and 13, provided that the eigenvalues and eigenfunctions are now found from the similarity transformation of $\mathbf{A}^{(x)}$ instead of $\mathbf{A}$ and N is replaced by N^x. This formulation presents the advantage of yielding the dispersion of relaxational modes. However, it is clear that determination of the eigenvalues of $\mathbf{A}^{(x)}$ becomes prohibitively time-consuming for $x \ge 3$. The orientational correlation functions in this case are preferably computed by a recently developed[23,24] matrix multiplication scheme.

Matrix Multiplication Scheme for the Calculation of Orientational Correlations. Let us consider the orientational correlation betwen two vectors $\mathbf{m}$ and $\mathbf{n}$ affixed to the ith and jth bonds relative to the frame OXYZ. Let us assume that $i \le j \le n$. The equality $i = j$ holds for the case of orientational *autocorrelation*. Following the conventional approach,[25] the axes of the local bond-based frame are defined according to the prescription given above for the first bond of the kinetic segment. For a given configurational transition from state $\{\Phi\}$ at time 0 to state $\{\Phi\}'$ at time t, the scalar product $\mathbf{m}(0)\cdot\mathbf{n}(t)$ may be written as

$$\mathbf{m}(0)\cdot\mathbf{n}(t) = \mathbf{T}\{\Phi\}\mathbf{m}^\circ\cdot\mathbf{T}\{\Phi\}'\mathbf{n}^\circ = \mathbf{m}^{\circ T}[\mathbf{T}^T\{\Phi\}\,\mathbf{T}\{\Phi\}']\mathbf{n}^\circ \tag{17}$$

where $\mathbf{T}\{\Phi\}$ and $\mathbf{T}\{\Phi\}'$ are the frame transformation operators to express both vectors in the frame OXYZ and $\mathbf{m}^\circ$ and $\mathbf{n}^\circ$ are the dipole vectors expressed in the bond coordinate system. They are given by the serial multiplication of the transformation matrices $\mathbf{T}_k(t)$ associated with the passage from local frame $k+1$ to frame k according to

$$\mathbf{T}\{\Phi\} = \prod_{k=1}^{i} \mathbf{T}_k(0) \qquad \mathbf{T}\{\Phi\}' = \prod_{k=1}^{j} \mathbf{T}_k(t) \tag{18}$$

The arguments account for the implicit time dependence of the torsional angle ϕ_k present in $\mathbf{T}_k(t)$. The ensemble average of eq 17 over all possible configurational transitions may be obtained[24] from

$$\langle \mathbf{m}(0)\cdot\mathbf{m}(t)\rangle = \mathbf{m}^{\circ T}(\mathbf{D}(t) \otimes \mathbf{E}_3)(\mathbf{E}_3 \otimes \mathbf{F})\mathbf{m}^\circ \tag{19}$$

Here, $\mathbf{E}_3$ is the identity matrix of order 3, $\mathbf{F} \equiv$ col (1 0 0 0 1 0 0 0 1), the symbol $\otimes$ represents the direct product, the superscript T indicates the transpose, and the matrix $\mathbf{D}(t)$ is defined as

$$\mathbf{D}(t) \equiv \mathbf{F}^T\left\langle \prod_{k=1}^{j} [\mathbf{T}_k(0) \otimes \mathbf{T}_k(t)] \right\rangle \tag{20}$$

In eq 20, $\mathbf{T}_k(0)$ is set equal to $\mathbf{E}_3$, for $k > i$. The product $\langle \prod_{k=1}^{j} [\mathbf{T}_k(0) \otimes \mathbf{T}_k(t)] \rangle$ is conveniently found for pairwise interdependent bonds, using the matrix multiplication scheme

$$\left\langle \prod_{k=1}^{j} [\mathbf{T}_k(0) \otimes \mathbf{T}_k(t)] \right\rangle = (\mathbf{J}^T \otimes \mathbf{E}_9) \times \prod_{k=2}^{j} [(\mathbf{V}_k(t) \otimes \mathbf{E}_9)\|\mathbf{T}_k \otimes \mathbf{T}_k\|]\ (\mathbf{J} \otimes \mathbf{E}_9) \tag{21}$$

Here, $\mathbf{J} \equiv$ col (1 1 ... 1) and $\mathbf{V}_k(t)$ is the stochastic weight matrix corresponding to the pair of bonds $(k-1, k)$.[23,24] It is noted that the first bond of the kinetic segment is not considered. The latter prescribes the absolute orientation of the kinetic segment and does not affect the internal orientational correlations. $\|\mathbf{T}_k \otimes \mathbf{T}_k\|$ is the diagonal supermatrix of the form

$$\|\mathbf{T}_k \otimes \mathbf{T}_k\| = \begin{bmatrix} \mathbf{T}_\alpha \otimes \mathbf{T}_\alpha & & & \\ & \mathbf{T}_\alpha \otimes \mathbf{T}_\beta & & \\ & & \dots & \\ & & & \mathbf{T}_\zeta \otimes \mathbf{T}_\zeta \end{bmatrix}_k \tag{22}$$

where $\mathbf{T}_\alpha$, $\mathbf{T}_\beta$, ..., $\mathbf{T}_\zeta$ are the forms assumed by the transformation matrix for the respective states $\alpha, \beta, \dots, \zeta$ assumed by bond k.

For the particular case of a kinetic segment of $x = n/4$ repeat units in *cis*-PIP, confining attention to the orien-

tational autocorrelation of the nth bond based frame, eq 21 is replaced by the simpler expression

$$\left\langle \prod_{k=1}^{n} [\mathbf{T}_k(0) \otimes \mathbf{T}_k(t)] \right\rangle = \prod_{p=1}^{x} \langle \mathbf{T}^*_p(0) \otimes \mathbf{T}^*_p(t) \rangle = \prod_{p=1}^{x} [(\mathbf{V}^*_p(t) \otimes \mathbf{E}_9) \| \mathbf{T}^*_p \otimes \mathbf{T}^*_p \| (\mathbf{J} \otimes \mathbf{E}_9)] \quad (23)$$

Here, $\mathbf{T}^*_p$ is the transformation matrix that operates between successive repeat units p and $p+1$. It is given by $\mathbf{T}^*_p \equiv \mathbf{T}_1\mathbf{T}_2\mathbf{T}_3\mathbf{T}_4$, following the index notation of Figure 1. The first equality in eq 23 follows from the intramolecular energetic considerations. For a total of N states accessible to each of the repeat units, the stochastic weights associated with the N^2 rotameric transitions equate to the time-delayed joint probabilities $P_{\alpha\beta}(t)$ for states α and β and are organized in $\mathbf{V}^*_p(t)$ as

$$\mathbf{V}^*_p(t) = \text{row}\,[P_{11}(t), P_{12}(t), P_{13}(t), ..., P_{NN}(t)]_p \quad (24)$$

The subscript p appended to the above row indicates that the time-delayed joint probabilities are dependent on the location of the specific unit p along the kinetic segment of x repeat units.

Dipole Moment Correlation Function. Let us assume that there are x dipole moments in a kinetic segment that is observed by the dielectric measurements at a given frequency and temperature. The dipole moment correlation function or the normalized response function $\Phi(t)$ is given by

$$\Phi(t) = \frac{\sum_{(s)=1}^{x}\sum_{(r)=1}^{x} [\langle \mathbf{m}_{(s)}(t)\cdot\mathbf{m}_{(r)}(0)\rangle - \langle \mathbf{m}_{(s)}(0)\rangle\cdot\langle \mathbf{m}_{(r)}(0)\rangle]}{\sum_{(s)=1}^{x}\sum_{(r)=1}^{x} [\langle \mathbf{m}_{(s)}(0)\cdot\mathbf{m}_{(r)}(0)\rangle - \langle \mathbf{m}_{(s)}(0)\rangle\cdot\langle \mathbf{m}_{(r)}(0)\rangle]} \quad (25)$$

where $\mathbf{m}_{(s)}(t)$ denotes the dipole moment located at the sth repeat unit of the kinetic segment with respect to the frame of observation OXYZ. The brackets indicate the ensemble averaging over all configurational transitions at the given time. The orientational autocorrelation $\langle \mathbf{m}_{(s)}(t)\cdot\mathbf{m}_{(s)}(0)\rangle$ is evaluated by combining eqs 19, 20, and 23 as

$$\langle \mathbf{m}_{(s)}(t)\cdot\mathbf{m}_{(s)}(0)\rangle\, \mathbf{m}^{\circ T} \times \left(\left\{ \mathbf{F}^T \prod_{p=1}^{s} [(\mathbf{V}^*_p(t) \otimes \mathbf{E}_9) \| \mathbf{T}^*_p \otimes \mathbf{T}^*_p \| (\mathbf{J} \otimes \mathbf{E}_9)] \right\} \otimes \mathbf{E}_3 \right) \times (\mathbf{E}_3 \otimes \mathbf{F})\mathbf{m}^\circ \quad (26)$$

For clarity, we shall abbreviate the right side of the above equation as

$$\langle \mathbf{m}_{(s)}(t)\cdot\mathbf{m}_{(s)}(0)\rangle = \mathbf{m}^{\circ T}\langle \boldsymbol{T}_s(0)\, \boldsymbol{T}_s(t)\rangle \mathbf{m}^\circ \quad (27)$$

in the following. On the other hand, the repeat units being subject to independent conformational energies, the cross-correlation between consecutive dipoles along the chain reduces to

$$\langle \mathbf{m}_{(s)}(t)\cdot\mathbf{m}_{(s+1)}(0)\rangle = \mathbf{m}^{\circ T}\langle \boldsymbol{T}_s(0)\, \boldsymbol{T}_s(t)\rangle \langle \mathbf{T}^*\rangle \mathbf{m}^\circ \quad (28)$$

Here, $\langle \mathbf{T}^*\rangle$ is the equilibrium average of the product of transformation matrices for the repeat unit. Using eqs 27 and 28 and neglecting cross-correlations beyond first-neighbor dipoles, eq 25 may be expressed for $x = 3$ as

$$\Phi(t) = \frac{\mathbf{G}(t) - \mathbf{G}(\infty)}{\mathbf{G}(0) - \mathbf{G}(\infty)} \quad (29)$$

where

$$\mathbf{G}(t) \equiv \mathbf{m}^{\circ T}\langle \boldsymbol{T}_1(0)\, \boldsymbol{T}_1(t) + \boldsymbol{T}_2(0)\, \boldsymbol{T}_2(t)\rangle(\mathbf{E}_3 + 2\langle \mathbf{T}^*\rangle) + \langle \boldsymbol{T}_3(0)\, \boldsymbol{T}_3(t)\rangle \mathbf{m}^\circ \quad (30)$$

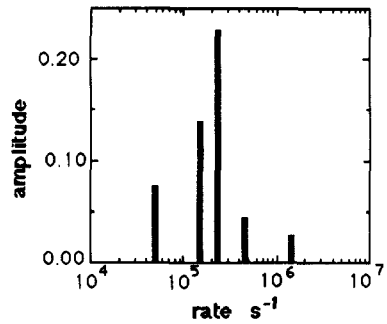

Figure 5. Eigenrates λ_ξ and their amplitudes k_ξ for a kinetic segment of one monomer unit. $\xi = 1$–12, in a homogeneous medium. Degenerate eigenrates and the zero eigenrate corresponding to equilibrium are not shown.

Calculations and Discussion

Calculations are performed for the temperature range $222.3 \le T \le 244.3$ K, studied in dielectric experiments.[6] Within this narrow interval, the variation of the equilibrium distribution of isomeric configurations with temperature is negligibly small. Thus, the exponential part of eq 10, which reflects the influence of short-range intramolecular energetics on transition rates, is not significantly affected. This insensitivity is manifested by the constant slope of the time decay curves at different temperatures. The only effect of temperature is to uniformly shift the correlation curves along the time axis. This effect arises primarily from the WLF type dependence of the front factor in eq 10 on temperature following the proportionality[20]

$$\log A_0(T) \propto \left[\frac{C_1(T - T_0)}{C_2 + T - T_0}\right] \quad (31)$$

where C_1, C_2, and T_0 for the segmental mode in *cis*-PIP in the bulk state are given by Boese and Kremer.[6] Thus, the parameters defining the WLF-type behavior of bulk PIP have been established in several experiments including the recently performed dielectric measurements. In this respect, our attention in the present work is directed to the interpretation of the slope of the decay curves. The two cases of a homogeneous and fluctuating environment will be considered separately.

(a) Relaxation in a Homogeneous Environment. Solution of the master equation leads to the determination of eigenrates and their amplitudes. The eigenrates $|\lambda_\xi|$ $(1 \le \xi \le N)$ indicate the rate of relaxation of the eigenmodes. They are directly found from the diagonalization of the transition rate matrix $\mathbf{A}$. Their amplitudes k_ξ are calculated from eq 13. The latter depends on the direction of the dipole moment vector in *cis*-PIP with respect to the bond-based local frame. The dipole vector lies in the xy plane of the local frame, though the angle it makes with the axes is not precisely known. The calculations reported in this study are based on a dipole perpendicular to the double bond. Calculations for various angles in the xy plane other than 90° indicate that results are not significantly altered. In Figures 5 and 6, dispersions of the eigen-

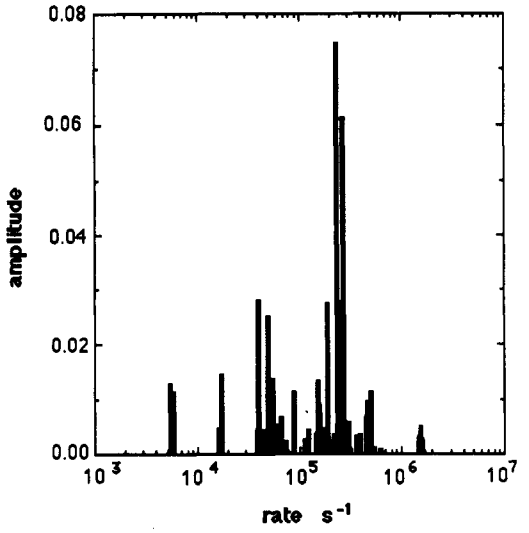

Figure 6. Eigenrates λ_ξ and their amplitudes k_ξ for a kinetic segment of two monomer units, in a homogeneous medium. ξ = 1–144. Degenerate eigenrates and the zero eigenrate corresponding to equilibrium are not shown.

rates are presented for kinetic segments of one and two repeat units, respectively, in a homogeneous environment. Results of calculations are reported for T = 240 K. The front factor in eq 13 is taken as 1.0×10^8/s. It is to be noted that the absolute value of the front factor scales the whole set of eigenrates by a constant factor, leaving their frequency distribution unchanged. Hence, the shape of the decay curve remains the same while only the time range of relaxation is uniformly shifted. Figure 5 is obtained for the dipole moment affixed to the fourth bond of a kinetic segment of one monomer unit, where the first bond is fixed in space. Only five out of twelve eigenrates appear in Figure 5 because some are degenerate. The zero eigenrate corresponding to equilibrium is not shown. The highest rate of 2×10^6 s^{-1} approaches the rate of transition of a single bond over the smallest energy barrier which is equal to 4.9×10^6 s^{-1}. The eigenrates cover a time span of approximately 1.5 decades. Figure 6 shows the eigenrates and amplitudes for a dipole moment attached to the end of two monomer units whose first bond is fixed in space. Only a fraction of the possible 144 eigenrates explicitly appears in the figure due to degeneracy. The frequency distribution of the eigenmodes is substantially broadened; eigenrates cover a time span of about 2.5 decades.

As the dispersion of the eigenrates widens, the shape of the response function is expected to depart from a single exponential and to approach the stretched exponential form expressed by eq 1. In Figures 7–9, results of calculations of the dipole autocorrelation functions of single dipoles are presented as a function of time for different length mobile sequences. In order to afford comparison with the stretched exponential function, the ordinate and abscissa of the figures are chosen as log (−ln Φ) and log t, respectively. All three figures show the presence of two distinct regimes that may be represented by two straight lines of different slopes. The circles represent results of calculations, and the straight lines are obtained by least-squares fit. Figure 7 is obtained for a kinetic sequence of one monomer unit with four bonds. The slope of the straight line at short times is 0.96. This portion of the diagram having a slope close to unity is representative of single exponential relaxation. The long time portion of the graph has a slope of 0.62, which indicates that a distribution of eigenrates contributes to

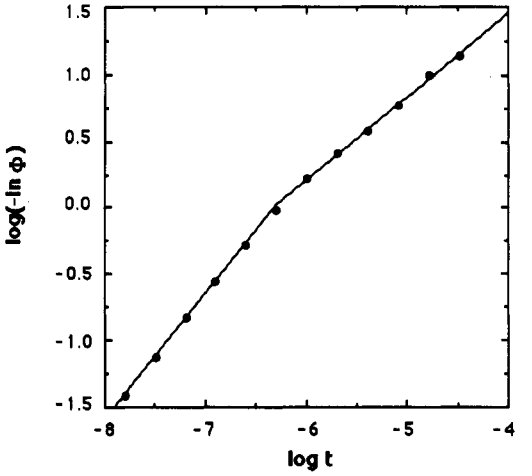

Figure 7. Dielectric response function for a dipole moment vector at the end of a kinetic segment of one monomer unit, in a homogeneous medium. The circles represent results of calculations. The two best fitting straight lines through the circles have slopes of 0.96 and 0.62, respectively, indicating approximately single exponential behavior followed by a KWW type relaxation at long times.

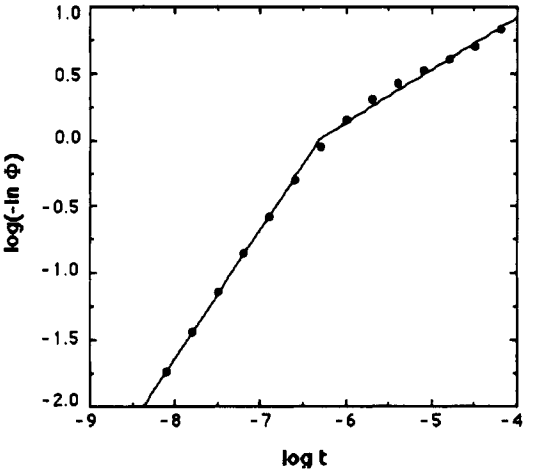

Figure 8. Dielectric response function for a dipole moment vector at the end of a kinetic segment of two monomer units, in a homogeneous medium. See legend for Figure 7. The best fitting straight lines have slopes of 0.97 and 0.39, respectively.

the relaxation at longer times. The two straight lines intersect when the ordinate equates approximately to zero. This indicates that stretched exponential type of relaxation is observed after the relaxation has fallen below its $1/e$ point. The value of the characteristic time τ of the stretched exponential function is obtained from the figure as 2.0×10^{-5} s when the ordinate equates to unity. Figure 8 is obtained for the autocorrelation function of a single dipole affixed to the end of the second monomer unit in a kinetic segment of two units. The slopes of the two straight lines are obtained as 0.97 and 0.39 representative of again a single exponent type decay at short times followed by a stretched exponent decay at longer times. Again, the latter starts after 60% of the full decay has taken place. The characteristic time is rather close to the preceding case. Finally, Figure 9 shows results of calculations of the autocorrelation function of a single dipole moment at the end of a kinetic sequence of three monomer units. The slopes of the two straight lines in the figure are 0.92 and 0.34, and same characteristic time is preserved. We note the gradual decrease in the exponent at long times, which is a direct consequence of the broader distribution of relaxation rates associated with longer kinetic segments. However, this exponent appears only toward the later

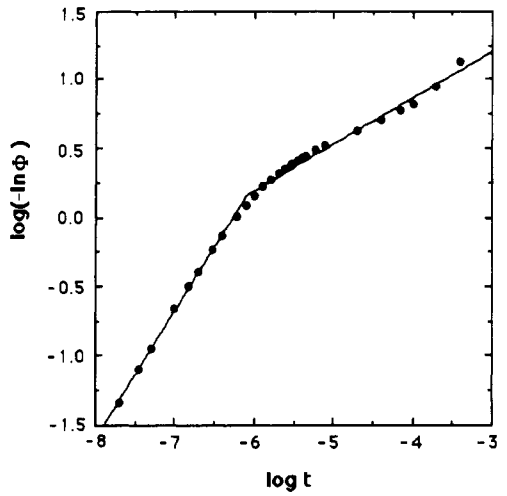

Figure 9. Dielectric response function for a dipole moment vector at the end of a kinetic segment of three monomer units, in a homogeneous medium. See legend for Figure 7. The best fitting straight lines have slopes of 0.92 and 0.34, respectively.

stages of relaxation, in contrast to experimental observations where stretched exponential behavior extends throughout the whole decay curve. The effect of fluctuations in the environment will be investigated next, as a possible source of observing a stretched exponential behavior throughout a wider time range.

Figures 7–9 are obtained for the relaxation of a single dipole moment affixed to the end of the kinetic segment. However, the dielectric relaxation experiment measures auto- and cross-contributions from all dipole moments in the kinetic segment. In a kinetic segment of two monomer units, for example, there are two dipole moments present and the response function must embody contributions from both of these dipoles. Calculations performed by considering the contributions from both auto- and cross-correlations of the dipoles on the fourth, eighth, and the twelfth bonds in a kinetic segment of three repeat units indicate that the response function exhibits approximately the same time dependence as the autocorrelation curve shown in Figure 9. Mainly, the bimodal character of the response function remains unchanged, and the corresponding time dependence on logarithmic scale is almost indistinguishable from that of the response function shown in Figure 9.

The above calculations demonstrate that, for a chain relaxing in a homogeneous environment, the KWW type behavior predicted by the theory is confined to the long time tail of the correlation decay curves only, in contrast to the experimental measurements which reveal a KWW type decay over the full range of relaxation. This deviation stipulates the necessity of broadening the frequency distribution of relaxational modes. This requirement may be achieved by allowing for a larger variety of accessible states and passages. Two possible pathways are either to consider longer kinetic segments or to introduce the density or free-volume fluctuations of the environment which modulate the rate of conformational transitions. The former is not expected to yield the required behavior in as much as in all of the three different sized kinetic units the single exponential behavior persists up to $1/e$ point of full relaxation. Besides, similar nonexponential decay is observed even in small molecules.[14-16] As to the exponent in the stretched exponential regime, it exhibits a steady decrease with increasing number of bonds engaged in cooperative relaxation. The exponents 0.39 and 0.34 obtained for the kinetic segments of two and three repeat

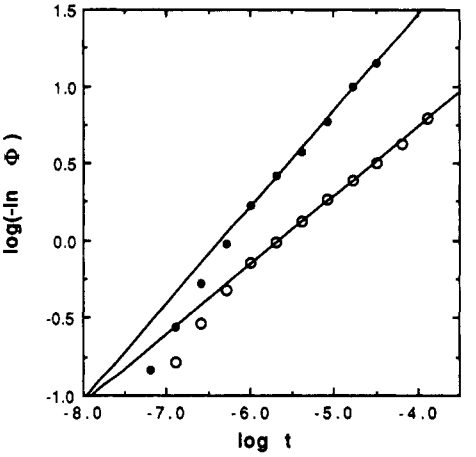

Figure 10. Dielectric response function for a kinetic segment of one monomer unit. Empty circles represent the results for the case of a kinetic segment relaxing in a bistate fluctuating environment. Results for a homogeneous environment are also shown by the filled circles, for comparison. The slope of the best fitting straight line through the final portion of the data is found to decrease from 0.62 to 0.45 upon inclusion of the fluctuating environment.

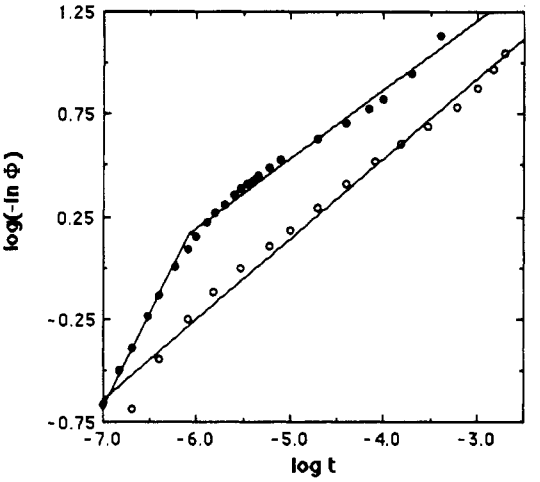

Figure 11. Dielectric response function for a kinetic segment of three monomer units. Empty and filled circles represent results in a bistable fluctuating environment and homogeneous media, respectively. The best fitting straight line drawn through the empty circles has slope equal to 0.39.

units, respectively, suggest that the consideration of larger size segments is unnecessary. At this point, the introduction of intermolecular effects associated with the density fluctuations of the environment seems appropriate.

(b) Relaxation in a Fluctuating Two-State Environment. To keep generality, we assign equal probabilities to the fast and slow environments, taking $p_{slow} = 0.5$ which leads from detailed balance principle to $r_{slow} = r_{fast}$. The decay curves equivalent to those in Figures 7 and 9, now in the presence of a fluctuating environment, are displayed by the empty circles in Figures 10 and 11, respectively. Results are reported for $r_{slow} = 1.0 \times 10^3$/s and $A_0 = 1.0 \times 10^9$/s. It is noted that since the rate of environmental transition $r_{slow} = r_{fast}$ is assumed to be much slower than the rate of isomeric transitions, the environment causes only the change in the effective friction coefficient, through the parameter g. The value of the parameter g will be selected so as to ensure sufficient broadening of the relaxation spectrum. For comparative purposes, the decay curves obtained in a homogeneous environment using the same front factor A_0 are also displayed, by the filled circles, in the figures.

For the simpler case of the kinetic segment of a single monomer unit, the two curves in Figure 10 are obtained from the application of the set of eqs 12 and 13, with the transition rate matrix therein taken as **A** for the homogeneous environment and as $\tilde{\mathbf{A}}$ for the fluctuating environment. The parameter g in eq 15 is taken as 0.01, which corresponds to a slowing of the motions by 2 orders of magnitude in the slow environment. From examination of Figure 10, two features brought about from environmental effects appear as (i) the lowering of the exponent β from 0.62 to 0.45, as found from the best fitting straight lines through the final portion of the data, and (ii) the extension of the stretched exponential behavior toward initial stages of relaxation, i.e., the validity of a KWW type relaxation starting from $\Phi \approx 0.6$, as found from log $(-\ln \Phi) \approx -0.3$ (empty circles), instead of $\Phi \approx 0.35$ (filled circles).

In the case of the longer kinetic segment of three repeat units presented in Figure 11, the matrix multiplication scheme described above is adopted since the large size of accessible transitions prohibits the use of the simpler set of eqs 12 and 13. The total number of transitions contributing to relaxation amount to 12^6 in the homogeneous medium and 24^6 in the presence of a bistate fluctuating environment. The parameter g is taken as 0.001 in this case. The change in the shape of the dipole relaxation function obtained by inclusion of density fluctuations in the medium is striking, even in the logarithmic scale of the figure. The curve for the fluctuating environment closely approximates a stretched exponential decay with exponent 0.39 in agreement with experiments, throughout a substantial portion of relaxation starting from $\Phi \approx 0.8$.

Conclusion

The present analysis demonstrates that consideration of intramolecular effects alone, in a homogeneous environment, leads to a stretched exponential decay of orientational correlations at long times, preceded by single exponential behavior during the initial stages of relaxation. Approximately $1/e$ point of full relaxation appears as the region where the passage from one regime to the other takes place. Here, intramolecular effects encompass both the specific short-range conformational energetics and the long-range resistance to motion due to chain connectivity; the role of the intermolecular constraints is represented by a mean-field effective frictional resistance increasing with the size of the kinetic segment. The resulting exponent β is found to decrease with the size of the kinetic segment engaged in the cooperative relaxation process. It equates to 0.62, 0.39, and 0.34 for kinetic segments of one, two, and three monomer units, respectively. The latter value closely approximates the experimental observation, though experiments indicate the validity of a stretched exponential behavior throughout the full range of relaxation. This type of behavior is theoretically approached when the single chain is allowed to relax in a heterogeneous fluctuating environment, instead of a homogeneous medium. Approximating the free-volume fluctuations in the medium by the existence of two distinct states, slow and fast, in the close neighborhood of the kinetic segment and studying the relaxation process of the kinetic segment subject to both type of effects, of intra- and intermolecular origins, satisfactorily explain the extension of the stretched exponential behavior over time scales of several orders of magnitude.

Acknowledgment. B.E. gratefully acknowledges the support of the Max-Planck Gesellschaft. Partial support by Bogazici University Research Fund Project No. 91-P0028 is gratefully acknowledged by I.B.

References and Notes

(1) Adachi, K.; Kotaka, T. *Macromolecules* **1984**, *17*, 120.
(2) Adachi, K.; Kotaka, T. *Macromolecules* **1985**, *18*, 466.
(3) Adachi, K.; Kotaka, T. *J. Mol. Liq.* **1987**, *36*, 75.
(4) Adachi, K.; Kotaka, T. *Macromolecules* **1988**, *21*, 157.
(5) Imannishi, Y.; Adachi, K.; Kotaka, T. *J. Chem. Phys.* **1988**, *89*, 7585,7593.
(6) Boese, D.; Kremer, F. *Macromolecules* **1990**, *23*, 829.
(7) Williams, G. *Adv. Polym. Sci.* **1979**, *33*, 59.
(8) Stockmayer, W. H. *Pure Appl. Chem.* **1967**, *15*, 247.
(9) Hyde, P. D.; Ediger, M. D.; Kitano, T.; Ito, K. *Macromolecules* **1989**, *22*, 2253. Hyde, P. D.; Ediger, M. D. *J. Chem. Phys.* **1990**, *92*, 1036.
(10) Dejean de la Batie, R.; Laupretre, F.; Monnerie, L. *Macromolecules* **1989**, 22, 122.
(11) Skinner, J. L. *J. Chem. Phys.* **1983**, *79*, 1955; Budimir, J.; Skinner, J. L. *J. Chem. Phys.* **1985**, *82*, 5232.
(12) Fredrickson, G. H.; Brawer, S. A. *J. Chem. Phys.* **1986**, *84*, 3351.
(13) Brawer, S. A. *J. Chem. Phys.* **1984**, *81*, 954.
(14) Gerharz, B.; Meier, G.; Fischer, E. W. *J. Chem. Phys.* **1990**, *92*, 7110.
(15) Fischer, E. W. *Proceedings, Second International Workshop on Non-Crystalline Solids*, San Sebastian, Spain; Colmenero, J., Algria, A., Eds.; World Scientific: Singapore, 1990; p 172.
(16) Meier, G.; Gerharz, B.; Boese, D.; Fischer, E. W. *J. Chem. Phys.*, submitted for publication.
(17) Jernigan, R. L. In *Dielectric Properties of Polymers*; Karasz, F. E., Ed.; Plenum: New York, 1972; p 99.
(18) Bahar, I.; Erman, B. *Macromolecules* **1987**, *20*, 1368.
(19) Bahar, I.; Erman, B.; Monnerie, L. *Macromolecules* **1989**, *22*, 2396.
(20) Bahar, I.; Erman, B.; Monnerie, L. *Macromolecules* **1990**, *23*, 3805.
(21) Bahar, I.; Erman, B.; Monnerie, L. *Macromolecules* **1991**, *24*, 3618.
(22) Kloczkowski, A.; Mark, J. E.; Bahar, I.; Erman, B. *J. Chem. Phys.* **1990**, *92*, 4513.
(23) Bahar, I. *J. Chem. Phys.* **1989**, *91*, 6525.
(24) Bahar, I.; Mattice, W. L. *Macromolecules* **1990**, *23*, 2719.
(25) Flory, P. J. *Statistical Mechanics of Chain Molecules*; Interscience: New York, 1969. Reprinted by Hanser Publishers, Oxford University Press, 1989.
(26) Mark, J. E. *J. Am. Chem. Soc.* **1966**, *88*, 4354; **1967**, *89*, 6829.
(27) Abe, Y.; Flory, P. J. *Macromolecules* **1971**, *4*, 219.
(28) Abe, Y.; Flory, P. J. *Macromolecules* **1971**, *4*, 230.
(29) Fixman, M. *J. Chem. Phys.* **1978**, *69*, 1527, 1538.
(30) Anderson, J. E.; Ullman, R. *J. Chem. Phys.* **1967**, *47*, 2187.
(31) Cohen, M. H.; Grest, G. S. *Phys. Rev. B* **1979**, *20*, 1077.

Registry No. PIP (homopolymer), 9003-31-0.